



# Natural Convection Flow of Casson Fluid with Carbon Nanotubes Past an Accelerated Disk

Ahmad Qushairi Mohamad<sup>1</sup>(✉), Wan Nura'in Nabilah Noranuar<sup>1</sup>, Zaiton Mat Isa<sup>1</sup>,  
Sharidan Shafie<sup>1</sup>, Abdul Rahman Mohd Kasim<sup>2</sup>, Mohd Rijal Illias<sup>3</sup>,  
and Lim Yeou Jiann<sup>1</sup>

<sup>1</sup> Department of Mathematical Sciences, Faculty of Science, Universiti Teknologi Malaysia,  
81310 Johor Bahru, Johor, Malaysia

ahmadqushairi@utm.my

<sup>2</sup> Universiti Malaysia Pahang, Lebuhraya Tun Razak, 26300 Gambang, Kuantan, Pahang,  
Malaysia

<sup>3</sup> Centre of Mathematics Studies, Faculty of Computer and Mathematical Sciences, Universiti  
Teknologi MARA (UiTM), 40450 Shah Alam, Selangor, Malaysia

**Abstract.** In this study, the impact of heat transfer on free convective Casson nanofluid flow induced by an accelerated disk is analyzed. The study of non-Newtonian Casson nanofluid that is suspended by single wall carbon nanotubes (SWCNTs) and multi wall carbon nanotubes (MWCNTs) has a vital role in human blood flows. The problem is governed by governing momentum and energy equations that come along with appropriate conditions for initial and accelerated boundary. The dimensionless form of the governing equation is then derived by applying the suitable dimensionless variables. An exact solution of temperature and velocity fields is obtained by utilizing Laplace transform technique. The impacts of pertinent parameters such as Casson parameter, Grashof number, nanoparticle volume fraction and time on both profiles are discussed and illustrated graphically. It is found that both temperature and velocity distributions satisfyingly meet all the initial and boundary conditions. The addition of CNTs particles leads to an increase in both temperature and velocity profiles, and SWCNTs possess a higher magnitude of temperature due to its outstanding thermal conductivity when compared to MWCNTs.

**Keywords:** Casson Nanofluid · Accelerated Disk · Carbon Nanotubes · Laplace Transform

## 1 Introduction

The phenomenon of heat transfer has been widely found in many engineering and industrial applications, such as cooling systems of electric motors and generators, heat exchangers and turbine systems, as well as in the design of heating systems in buildings and vehicles. This main topic has attracted the significant interest of researchers

to investigate the process of heat transfer through a theoretical investigation, which can save cost and time of conducting experiments. Some recent studies on heat transfer by free convection with a viscous fluid along an oscillating plate were examined by Narahari et al. [1] and Rajput et al. [2]. Earlier work on the heat transfer process via Newtonian and non-Newtonian fluids with diverse geometries was conducted by Maqbool et al. [3], Rao et al. [4], and Prameela et al. [5]. Recently, most of the industrial applications such as bio-engineering processes, food processing industries, drilling operations, and metallurgy processes are encountered with non-Newtonian fluid. This type of fluid is found to be more complex compared to Newtonian fluid, and the simulation of the non-Newtonian fluid flow is significant for an industry to examine the heat transfer process [6]. This leads researchers to have a special interest in exploring the complexity of the non-Newtonian fluid model. A non-Newtonian physical behavior is commonly exhibited by substances that have an unfixed coefficient of viscosity, where the change in viscosity depends on the applied stress, such as cornstarch, paint, blood, honey, ketchup, and polymer solution. Casson fluid is a non-Newtonian fluid model that describes the flow behavior of a viscoplastic fluid, and it behaves like a shear thinning fluid when the applied stress dominates the flow. Once the level of applied stress surpasses the amount of the yield stress, fluid flow behavior is exhibited. In the present day, the rheological model for human blood is also described by Casson fluid due to the existence of several substances such as human red blood cell, globulin in aqueous, protein, fibrinogen, and base plasma [7]. Numerous studies on free convection of Casson fluid model have been conducted by considering various aspects, including [8–11]. Sandhya et al. [12] analyzed the mass and heat transfer on MHD Casson fluid flow across a moving porous plate under the influence of chemical reaction and radiation effects. Khan et al. [13] continued the work by including the effects of heat generation and Newtonian heating.

In addition, the efficiency of a heat transfer system is influenced by the fluid's thermal conductivity, whereby the heat transfer system would be more effective with the higher thermal conductivity. Conventional fluids (water and engine oil) have been shown to have restricted capabilities in heat transmission due to their low thermal conductivity. Therefore, Choi and Eastman [14] developed an engineered heat transfer fluid, known as nanofluid, in which nanoparticles such as metals, metal oxides, or carbon are suspended in a conventional fluid to enhance the thermal conductivity. Carbon nanotubes (CNTs) are among the developed nanoparticles and are often divided into two types. Material of single layer graphene sheet with diameter of less than 1 nm is called single wall carbon nanotubes (SWCNTs) while material of several multi-layer that concentrically interlinked graphene sheet with a diameter of more than 100 nm is called multi wall carbon nanotubes (MWCNTs). Khalid et al. [15] studied the impact of carbon nanotubes on free convection flow by considering water as the base fluid, and Khalid et al. [16] continued the previous work by replacing the base fluid with human blood. Both studies were solved for an oscillating boundary condition and the exact solutions were solved using the method of Laplace transform. Next, Ebaid et al. [17] used a stretching surface to conduct the same nanofluid study with the existence of a magnetic field effect, and the study revealed that the temperature and velocity distributions ascended with the addition of more nanoparticles to the base fluid. A similar work was done by Alkassasbeh et al. [18], considering both human blood and water and as base fluid, and their findings show

that increasing values of Casson nanofluid parameter results in a decreasing velocity profile and increasing temperature profile. Saqib et al. [19] investigated the nanofluid flow with a suspension of CNTs in Carboxy-Methyl-Cellulose (CMC) in two vertical parallel plates. It was concluded that MWCNTs nanoparticles exhibited higher velocity compared to SWCNTs nanoparticles due to their low density. Then, some related studies on heat transfer analysis were also conducted by [20, 21] but concentrated on the rotating convective flow of carbon nanotube nanofluid with radiation effect.

Based on the above review, the investigation of heat transfer analysis of carbon nanotubes nanofluid through the usage of accelerated boundary condition has not been investigated yet. However, the related study discovering the flow features of passing porous medium across a vertical accelerating plate was carried out by Chaudhary and Jain [22]. The extension of the previous problem was discussed by Hussain et al. [23], considering the effects of heat and mass transport. Mohamad et al. [24] used second grade fluid in conducting free convective flow which has been bounded to an accelerated plate and applied Laplace transform technique to generate the analytical solution of the temperature and velocity fields. The same method was used by Mohamad et al. [25] to solve the non-coaxial rotating flow through a porous medium for a viscous fluid over an accelerated plate. The study revealed that the acceleration parameter provides an enhancement in the fluid velocity. Several studies on accelerated boundary condition under the influence of various effects on the flow were done by researchers including [26–28]. From the literature, it is obviously seemed that the Casson nanofluid flow induced by an accelerating plate specifically using the mixture of carbon nanotubes in Casson human blood has not been found in any study. Therefore, motivated by this gap of study, the present work is carried out purposely to scrutinize the time-dependent natural convection flow of Casson nanofluid with carbon nanotubes over an accelerated disk. The closed form solution for temperature and velocity profiles with accelerated boundary condition is established using Laplace transform method. Both profiles are further analyzed for their parameters' effect with the help of graphical results together with a comprehensive discussion.

## 2 Problem Formulation

Consider an unsteady free convection flow of nanofluid past across a vertical accelerated disk as depicted in Fig. 1. Coordinate system is assumed in such way that  $x$ -axis is opted as along the plate in upward direction and  $z$ -axis is normal to plane of plate in the fluid. The flow is restricted with an accelerated disk at  $z = 0$  and the space  $z > 0$  is filled with Casson nanofluid of a constant kinematic viscosity  $\nu_{nf}$ . Two types of Casson nanofluid are considered such as the synthesis of human blood with SWCNTs and the synthesis of human blood with MWCNTs. Initially, at time  $t = 0$ , both disk and nanofluid are at rest and maintained at constant temperature  $T_\infty$ . Later, when  $t > 0$ , the disk starts to move with a constant acceleration  $A$  and the temperature of the plate is raised or lowered to  $T_w$ . The rheological equation (the relation of shear stress and strain rate) for an incompressible flow of a Casson fluid can be found in Khalid et al. [16].

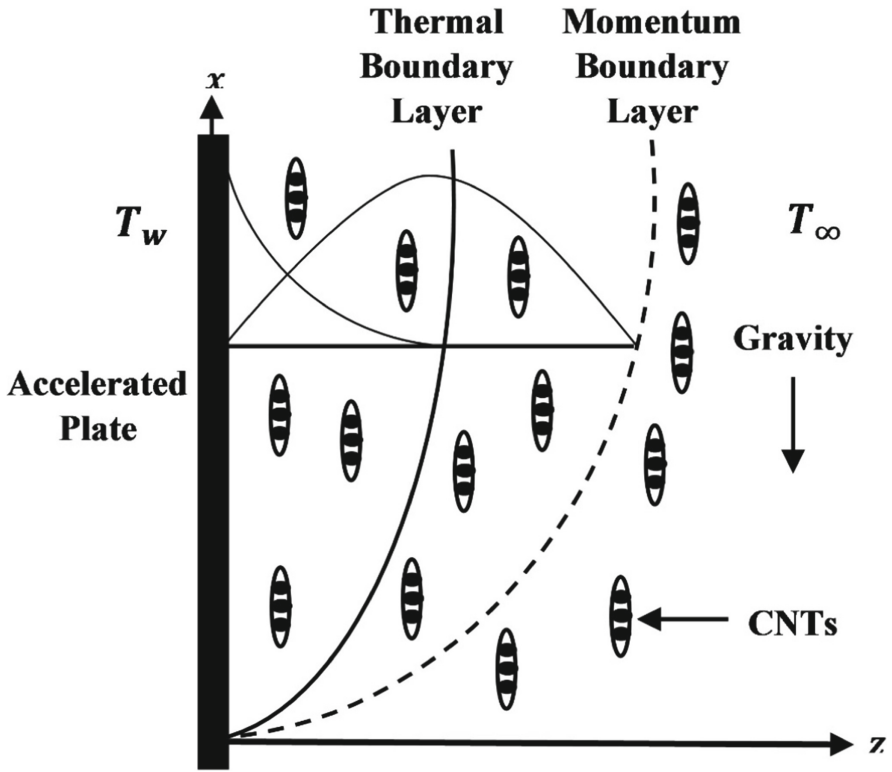


Fig. 1. Geometry of the problem.

Under the assumptions made above, the problem is governed by the governing equations which have been expressed by the adaptation of usual Boussinesq approximation and nanofluid model proposed by Tiwari and Das [29]. The momentum and energy equations take the form as

$$\rho_{nf} \frac{\partial u}{\partial t} = \mu_{nf} \left( 1 + \frac{1}{\gamma} \right) \frac{\partial^2 u}{\partial z^2} + g(\rho\beta)_{nf}(T - T_{\infty}), \tag{1}$$

$$(\rho C_p)_{nf} \frac{\partial u}{\partial t} = k_{nf} \frac{\partial^2 u}{\partial z^2}. \tag{2}$$

The initial and boundary conditions for the problem are

$$\begin{aligned} u(z, 0) &= 0, \quad T(z, 0) = T_{\infty}; \quad z > 0, \\ u(0, t) &= At, \quad T(0, t) = T_w; \quad t > 0, \\ u(\infty, t) &= 0, \quad T(\infty, t) = T_{\infty}; \quad t > 0, \end{aligned} \tag{3}$$

where  $u, T, k_{nf}, \mu_{nf}, \rho_{nf}, (C_p)_{nf}, \beta_{nf}$  are the velocity, temperature, thermal conductivity, dynamic viscosity, density, electrical conductivity, heat capacitance, thermal expansion coefficient for temperature specifically for Casson nanofluid. Another parameter

**Table 1.** Thermophysical features of Casson fluid, SWCNTs and MWCNTs.

Properties/Materials	Human blood	SWCNTs	MWCNTs
$\rho(Kgm^{-3})$	1053	2600	1600
$C_p(JKg^{-1}K^{-1})$	3594	425	796
$k(Wm^{-1}K^{-1})$	0.492	6600	3000
$\beta \times 10^{-5}(K^{-1})$	0.18	27	44

$\gamma = \mu \frac{\sqrt{2\pi c}}{p_y}$  and  $A$  are the Casson parameter and acceleration parameter. The nanofluid constant used in this study are written as

$$\begin{aligned} \mu_{nf} &= \frac{\mu_f}{(1-\phi)}, \beta_{nf} = \frac{(1-\phi)(\rho\beta)_f + \phi(\rho\beta)_{CNTs}}{\rho_{nf}}, \\ (\rho C_p)_{nf} &= (1-\phi)(\rho C_p)_f + \phi(\rho C_p)_{CNTs}, \\ \frac{k_{nf}}{k_f} &= \frac{1-\phi + 2\phi \frac{k_{CNTs}}{k_f} \ln \frac{k_{CNTs} + k_f}{2k_f}}{1-\phi + 2\phi \frac{k_f}{k_{CNTs} - k_f} \ln \frac{k_{CNTs} + k_f}{2k_f}}, \end{aligned} \tag{4}$$

where the thermal conductivity is adapted theoretically from Xue [30]. The constant  $\phi$  stands for solid volume fraction of nanofluid and the subscripts  $f$  and  $CNTs$  represent to fluid and carbon nanotubes. Here, the nanofluid constants defined in Eq. (4) are used based on their properties stated in Table 1.

Introducing the non-dimensional variables as follows

$$u^* = \frac{u}{(\nu A)^{\frac{1}{3}}}, z^* = \frac{zA^{\frac{1}{3}}}{\nu^{\frac{2}{3}}}, t^* = \frac{tA^{\frac{2}{3}}}{\nu^{\frac{1}{3}}}, T^* = \frac{T - T_\infty}{T_w - T_\infty} \tag{5}$$

and these variables collaborating with Eq. (4) are employed into the system of governing equations, Eq. (1) to Eq. (3). Thus, the system of equations is reduced to

$$\frac{\partial u}{\partial t} = \frac{1}{\phi_1} \left( 1 + \frac{1}{\gamma} \right) \frac{\partial^2 u}{\partial z^2} + Gr\phi_3 T, \tag{6}$$

$$\frac{\partial T}{\partial t} = \frac{\lambda}{Pr\phi_4} \frac{\partial^2 T}{\partial z^2} \tag{7}$$

with the conditions

$$\begin{aligned} u(z, 0) &= 0, T(z, 0) = 0; z > 0, \\ u(0, t) &= t, T(0, t) = 1; t > 0, \\ u(\infty, t) &= 0, T(\infty, t) = 0; t > 0, \end{aligned} \tag{8}$$

where

$$\begin{aligned} Pr &= \frac{\nu_f (\rho C_p)_f}{k_f}, Gr = \frac{g \beta_f (T_w - T_\infty)}{A}, \lambda = \frac{k_{nf}}{k_f}, \\ \phi_1 &= (1 - \phi)^{2.5} \left( (1 - \phi) + \frac{\phi \rho_{CNTs}}{\rho_f} \right), \\ \phi_3 &= \frac{(1 - \phi) + \frac{\phi (\rho \beta)_{CNTs}}{(\rho \beta)_f}}{(1 - \phi) + \frac{\phi \rho_{CNTs}}{\rho_f}}, \phi_4 = (1 - \phi) + \frac{\phi (\rho C_p)_{CNTs}}{(\rho C_p)_f}. \end{aligned} \tag{9}$$

Here,  $Pr$  and  $Gr$  are Prandtl number and Grashof number while for others are the constant parameters particularly for nanofluid.

### 3 Numerical Solution

On the use of Laplace transform method, the following governing equations in Ordinary Differential Equations (ODE) are formed as

$$\frac{d^2 \bar{u}}{dz^2} - a_1 q \bar{u} = -a_1 \phi_3 Gr \bar{T}, \tag{10}$$

$$\bar{u}(0, q) = \frac{1}{q^2}, \bar{u}(\infty, q) = 0, \tag{11}$$

$$\frac{d^2 \bar{T}}{dz^2} - b_0 q \bar{T} = 0, \tag{12}$$

$$\bar{T}(0, q) = \frac{1}{q}, \bar{T}(\infty, q) = 0. \tag{13}$$

After that, in order to solve Eq. (10) and Eq. (12), the condition for boundary in Eq. (11) and Eq. (13) are used. The resulting solution is then imposed with the inverse Laplace and results the following solutions for velocity and temperature

$$\begin{aligned} u(z, t) &= -b_1 \left[ \left( \frac{b_0 z^2}{2} + t \right) \operatorname{erfc} \left( \frac{-z \sqrt{b_0}}{2 \sqrt{t}} \right) \right] - b_1 \left[ \frac{z \sqrt{b_0 t}}{\sqrt{\pi}} \exp \left( \frac{-b_0 z^2}{4t} \right) \right] \\ &+ b_2 \left[ \left( \frac{a_1 z^2}{2} + t \right) \operatorname{erfc} \left( \frac{-z \sqrt{a_1}}{2 \sqrt{t}} \right) \right] + b_2 \left[ \frac{z \sqrt{a_1 t}}{\sqrt{\pi}} \exp \left( \frac{-a_1 z^2}{4t} \right) \right], \end{aligned} \tag{14}$$

$$T(z, t) = \operatorname{erfc} \left( \frac{z}{2} \sqrt{\frac{b_0}{t}} \right), \tag{15}$$

where

$$b_0 = \frac{Pr \phi_4}{\lambda}, b_1 = \frac{a_1 Gr \phi_3}{b_0 - a_1}, b_2 = 1 + b_1, a_0 = \frac{\gamma}{1 + \gamma}, a_1 = a_0 \phi_1. \tag{16}$$

### 4 Results and Discussion

To give the best insight into the flow regime of the considered problem, the velocity and temperature profiles are graphically plotted under the influence of embedded parameters with different numerical values such as Casson parameter  $\gamma$ , Grashof number  $Gr$ , the nanoparticle volume fraction of CNTs  $\phi$  and time  $t$ . The effects on the temperature and velocity fields are comprehensively discussed using the image discussion illustrated in Fig. 2 to Fig. 7. From these plots, all the results satisfactorily satisfied both initial and boundary conditions. The numerical Gaver-Stehfest algorithm [31, 32] is used to verify the accuracy of the generated solution, and good agreement is found when the comparison of the exact solution and the numerical Gaver-Stehfest algorithm yields an identical value, as clearly shown in Table 2. Thus, the validity is confirmed.

The influence of  $\gamma$  on the physical behavior of the velocity can be observed in Fig. 2. It should be noted that the Casson fluid is a viscoplastic fluid where the changes in  $\gamma$  affect the non-Newtonian behavior. In this figure, the effect of a large  $\gamma$  is accompanied by an increase in the plasticity of the fluid and leads to a decrease in the thickness of the velocity boundary layer. This flow regime can be justified by the Casson fluid study of Khan et al. [13] and Khalid et al. [16]. Figure 3 displays the impact of  $Gr$  on the velocity profile of human blood with suspended SWCNTs and MWCNTs. The graph shows that increasing the  $Gr$  values lead to an increase in velocity. This fluid behavior is caused by the temperature difference, which usually causes a decrease in density and leads to the buoyancy force acting on the flow to prevail. Therefore, it can accelerate the flow of nanofluids. A similar effect of  $Gr$  on velocity can be found in Khalid et al. [10].

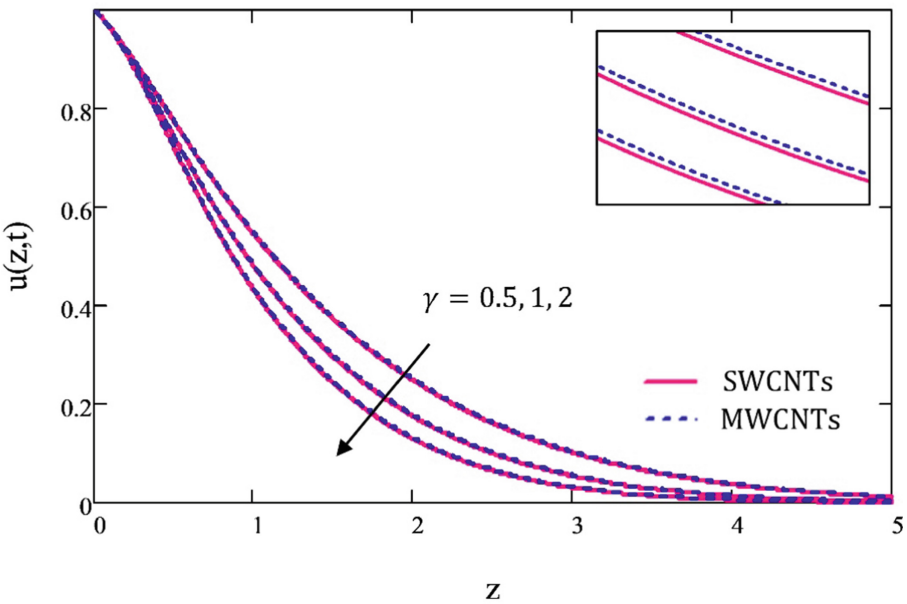
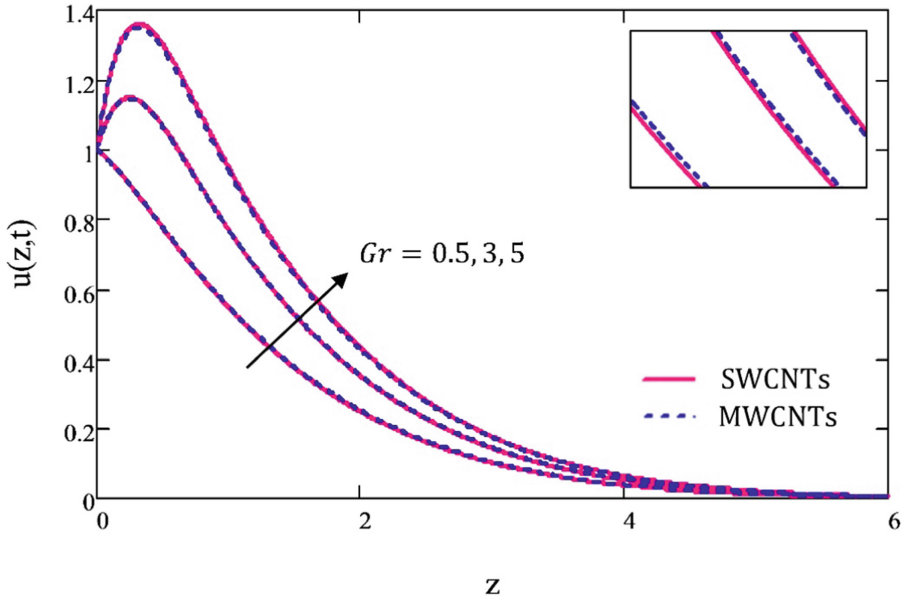


Fig. 2. Effect of  $\gamma$  on velocity profiles



**Fig. 3.** Effect of  $Gr$  on velocity profiles.

**Table 2.** Accuracy between exact solution and numerical Gaver-Stehfest algorithm for SWCNTs and MWCNTs with  $\gamma = 0.5$ ,  $Gr = 0.5$ ,  $\phi = 0.2$ ,  $t = 1$ ,  $Pr = 21$

z	Velocity			
	SWCNTs		MWCNTs	
	Exact	Gaver-Stehfest	Exact	Gaver-Stehfest
0	1.0000	1.0000	1.0000	1.0000
1	0.5459	0.5459	0.5486	0.5486
2	0.2480	0.2480	0.2514	0.2514
3	0.1012	0.1012	0.1037	0.1037
4	0.0368	0.0368	0.0382	0.0382
5	0.0119	0.0119	0.0125	0.0125
6	0.0034	0.0034	0.0036	0.0036

Next, the identical effect on the velocity and temperature distributions are observed with different values of  $\phi$ , as shown in Figs. 4 and 5, where both profiles exhibit an increasing trend as the value of  $\phi$  increases. The increasing velocity profile in Fig. 4, which is due to the addition of carbon nanotube nanoparticles to human blood may offer several advantages in the health field, particularly in the development of a drug delivery process that assists the transport of drugs directly to cancer growth and to areas of damaged arteries in the fight against cardiovascular disease. In heat transfer analysis,

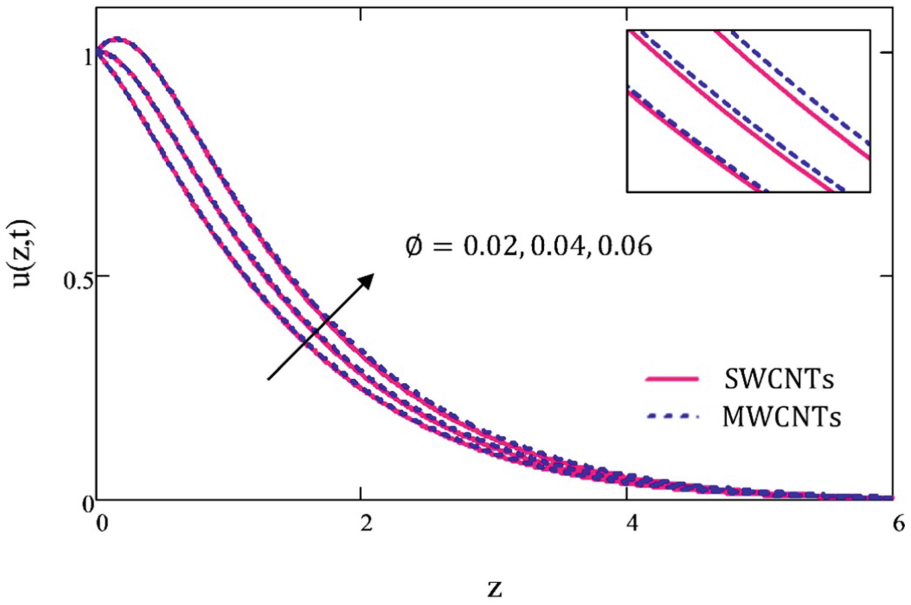


Fig. 4. Effect of  $\phi$  on velocity profiles.

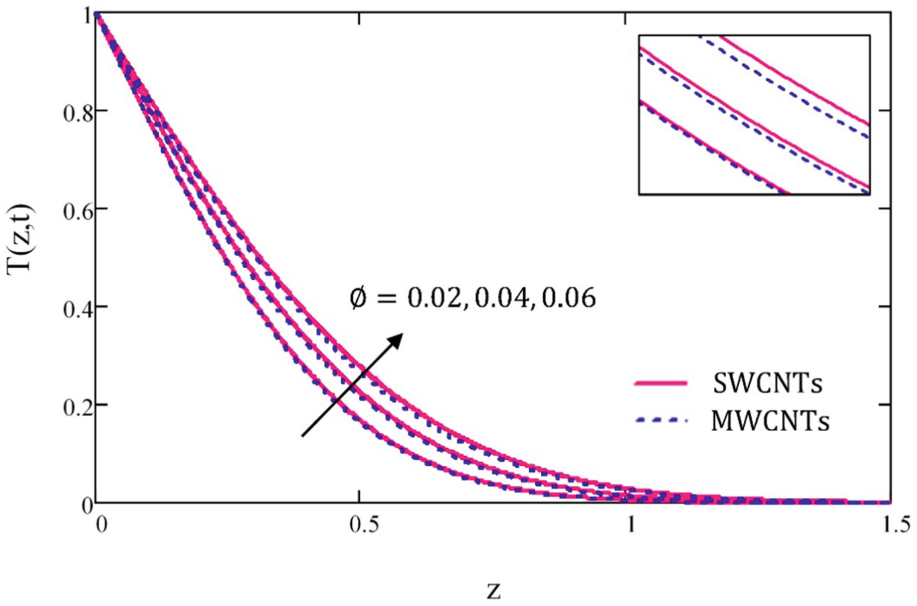
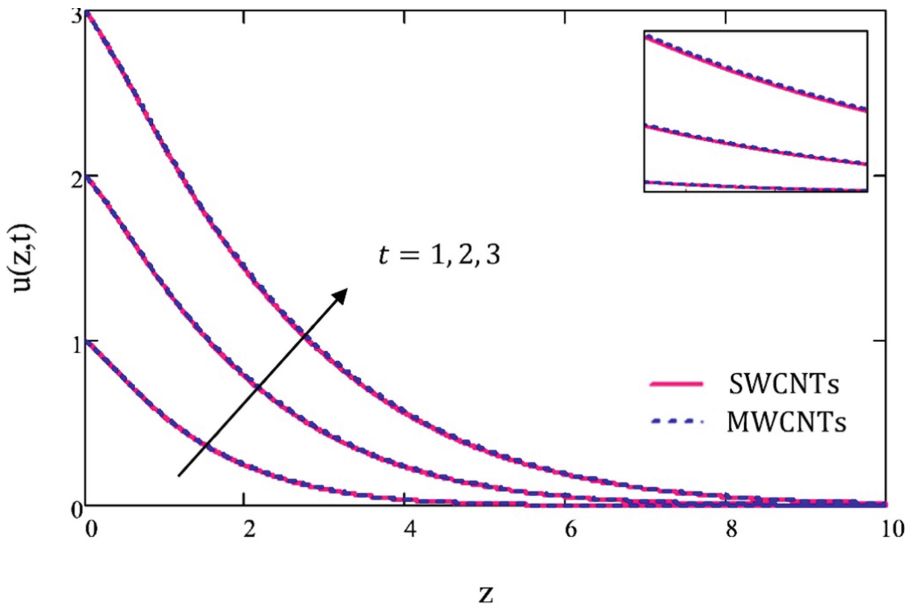


Fig. 5. Effect of  $\phi$  on temperature profiles.



**Fig. 6.** Effect of  $t$  on velocity profiles.

the use of greater carbon nanotubes volume fraction  $\phi$  causes the nanofluid to have high thermal conductivity, making heat conduction much more effective and also increasing the temperature of the nanofluid, as shown in Fig. 5. Ebaid et al. [17] also reported similar impacts of CNTs on temperature and velocity profiles.

After that, Figs. 6 and 7 depict the effects of different values of  $t$  on velocity and temperature profiles. The findings reveal that as the value of  $t$  increases, the velocity and temperature profiles of human blood with SWCNTs and MWCNTs also increase. This is because the buoyancy force can provide external energy sources for the flow over a longer period, so that the nanofluid flows at high velocity and the temperature of the nanofluid raises. From Figs. 2, 3, and 4, it is noticed that human blood with MWCNTs shows outstanding effect compared to SWCNTs because MWCNTs have low density of nanofluid, which leads to high velocity. However, Fig. 5 shows that the temperature of human blood increases significantly more in the presence of SWCNTs than in the presence of MWCNTs, which is due to the high thermal conductivity of SWCNTs that enables them to conduct more heat.

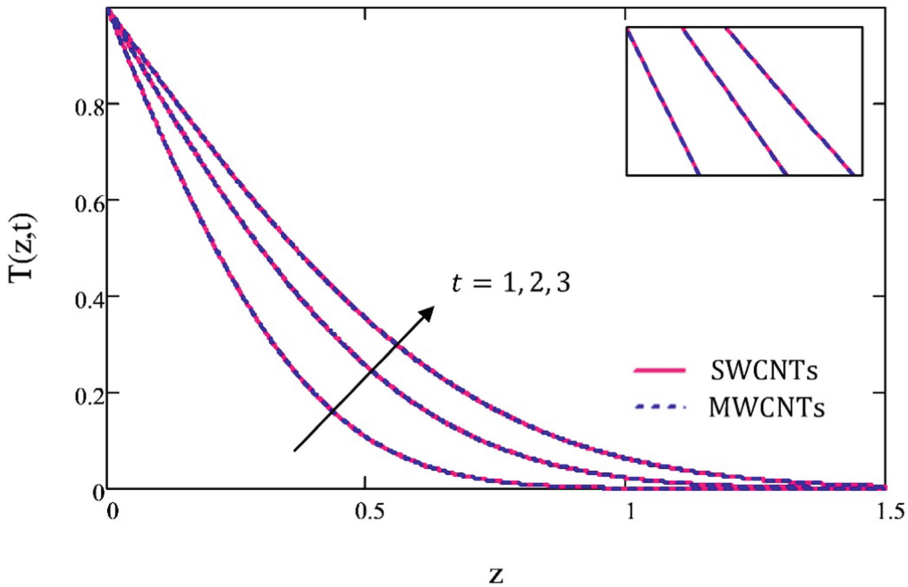


Fig. 7. Effect of  $t$  on temperature profiles.

## 5 Conclusion

Using Laplace transform method, the exact solution for the accelerated free convective flow of dispersed carbon nanotubes (CNTs) in human blood Casson fluid and heat transfer is achieved. The effect of several values of Casson parameter  $\gamma$ , Grashof number  $Gr$ , nanoparticles volume fraction  $\phi$  and time  $t$  on the velocity and temperature profiles are visually shown in graphs, and their physical behavior is discussed in detail. The following are the main findings of this study:

1. The velocity profile for both MWCNTs and SWCNTs amplifies with the rising values of  $Gr$ ,  $\phi$  and  $t$  but diminishes with rising values of  $\gamma$ .
2. The temperature profile for both MWCNTs and SWCNTs increases with the rising values of  $\phi$  and  $t$ .
3. Under the influence of  $\phi$ ,  $Gr$ , and  $\gamma$ , the velocity of human blood with MWCNTs are greater than SWCNTs while the temperature of human blood with SWCNTs is greater than MWCNTs.

## References

1. Narahari, M., Tippa, S., Pendyala, R., Fetecau, C.: Soret, heat generation, radiation and porous effects on MHD free convection flow past an infinite plate with oscillating temperature. *J. Therm. Anal. Calorim.* **143**(3), 2525–2543 (2020). <https://doi.org/10.1007/s10973-020-10229-5>

2. Rajput, U.S., Shareef, M.: MHD free convective flow along vertical oscillatory plate with radiative heat transfer in the presence of hall current and heat source. *J. Math. Fundam. Sci.* **51**(3), 252–264 (2019). <https://doi.org/10.5614/j.math.fund.sci.2019.51.3.4>
3. Maqbool, K., Sohail, A., Mann, A.B.: Numerical study of heat transfer and Hall current effects on the flow of Johnson-Segalman fluid between two eccentric rotating disks. *J. Phys. Commun.* **2**(5), 055017 (2018). <https://doi.org/10.1088/2399-6528/aac2a1>
4. Rao, S.R., Vidyasagar, G., Deekshitulu, G.V.S.R.: Unsteady MHD free convection Casson fluid flow past an exponentially accelerated infinite vertical porous plate through porous medium in the presence of radiation absorption with heat generation/absorption. *Mater. Today: Proc.* **42**(3), 1608–1616 (2021). <https://doi.org/10.1016/j.matpr.2020.07.554>
5. Prameela, M., Gangadhar, K., Reddy, G.J.: MHD free convective non-Newtonian Casson fluid flow over an oscillating vertical plate. *Partial Differ. Equ. Appl. Math.* **5**, 100366 (2022). <https://doi.org/10.1016/j.padiff.2022.100366>
6. Aneja, M., Chandra, A., Sharma, S.: Natural convection in a partially heated porous cavity to Casson fluid. *Int. Commun. Heat Mass Transfer* **114**, 10455 (2020). <https://doi.org/10.1016/j.icheatmasstransfer.2020.104555>
7. Anwar, T., Kumam, P., Waththayu, W.: Unsteady MHD natural convection flow of Casson fluid incorporating thermal radiative flux and heat injection/suction mechanism under variable wall conditions. *Sci. Rep.* **11**, 4275 (2021). <https://doi.org/10.1038/s41598-021-83691-2>
8. Mohamad, A.Q., Jaafar, N.A., Shafie, S., Ismail, Z., Qasim, M.: Theoretical study on rotating Casson fluid in moving channel disk. *J. Phys: Conf. Ser.* **1366**, 012039 (2019). <https://doi.org/10.1088/1742-6596/1366/1/012039>
9. Hussanan, A., Salleh, M.Z., Khan, I., Shafie, S.: Analytical solution for suction and injection flow of a viscoplastic Casson fluid past a stretching surface in the presence of viscous dissipation. *Neural Comput. Appl.* **29**(12), 1507–1515 (2016). <https://doi.org/10.1007/s00521-016-2674-0>
10. Khalid, A., Khan, I., Khan, A., Shafie, S.: Unsteady MHD free convection flow of Casson fluid past over an oscillating vertical plate embedded in a porous medium. *Eng. Sci. Technol. Int. J.* **18**(3), 309–317 (2015). <https://doi.org/10.1016/j.jestch.2014.12.006>
11. Kataria, H.R., Patel, H.R.: Heat and mass transfer in magnetohydrodynamic (MHD) Casson fluid flow past over an oscillating vertical plate embedded in porous medium with ramped wall temperature. *Propuls. Power Res.* **7**(3), 257–267 (2018). <https://doi.org/10.1016/j.jprr.2018.07.003>
12. Sandhya, A., Reddy, G., Deekshitulu, V.S.R.: Radiation and chemical reaction effects on MHD Casson fluid flow past a semi-infinite vertical moving porous plate. *Indian J. Pure Appl. Phys.* **58**(7), 548–557 (2020)
13. Khan, D., Khan, A., Khan, I., Ali, F., ul Karim, F., Tlili, I.: Effects of relative magnetic field, chemical reaction, heat generation and Newtonian heating on convection flow of Casson Fluid over a moving vertical plate embedded in a porous medium. *Sci. Rep.* **9**(1), 1–18 (2019). <https://doi.org/10.1038/s41598-018-36243-0>
14. Choi, S.U.S., Eastman, J.A.: *Enhancing Thermal Conductivity of Fluids with Nanoparticles*, United State (1995)
15. Khalid, A., Jiann, L.Y., Khan, I., Shafie, S.: Exact solutions for unsteady free convection flow of carbon nanotubes over an oscillating vertical plate. *AIP Conf. Proc.* **1830**(1), 020054 (2017). <https://doi.org/10.1063/1.4980917>
16. Khalid, A., Khan, I., Khan, A., Shafie, S., Tlili, I.: Case study of MHD blood flow in a porous medium with CNTS and thermal analysis. *Case Stud. Thermal Eng.* **12**, 374–380 (2018). <https://doi.org/10.1016/j.csite.2018.04.004>
17. Ebaid, A., Al Sharif, M.A.: Application of Laplace transform for the exact effect of a magnetic field on heat transfer of carbon nanotubes-suspended nanofluids. *Z. Naturforsch.* **70**(6), 471–475 (2015)

18. Alkassabbeh, H.T., Swalmeh, M.Z., Saeed, H.G.B., Al Faqih, F.M., Talafha, A.G.: Investigation on CNTs-water and human blood based Casson nanofluid flow over a stretching sheet under impact of magnetic field. *Front. Heat Mass Transfer* **14**, 1–7 (2020). <https://doi.org/10.5098/hmt.14.15>
19. Saqib, M., Khan, I., Shafie, S.: Application of Atangana-Baleanu fractional derivative to MHD channel flow of CMC-based-CNT's nanofluid through a porous medium. *Chaos Solitons Fractals* **116**, 79–85 (2018). <https://doi.org/10.1016/j.chaos.2018.09.007>
20. Mosayebidorcheh, S., Hatami, M.: Heat transfer analysis in carbon nanotube-water between rotating disks under thermal radiation conditions. *J. Mol. Liq.* **240**, 258–267 (2017). <https://doi.org/10.1016/j.molliq.2017.05.085>
21. Dawar, A., Shah, Z., Islam, S., Idress, M., Khan, W.: Magnetohydrodynamic CNTs Casson nanofluid and radiative heat transfer in a rotating channels. *Int. J. Phys. Res. Appl.* **1**, 17–32 (2018)
22. Chaudhary, R.C., Jain, A.: An exact solution of magnetohydrodynamic convection flow past an accelerated surface embedded in a porous medium. *Int. J. Heat Mass Transf.* **53**(7), 1609–1611 (2010). <https://doi.org/10.1016/j.ijheatmasstransfer.2009.12.002>
23. Hussain, S.M., Jain, J., Seth, G.S., Rashidi, M.M.: Free convective heat transfer with hall effects, heat absorption and chemical reaction over an accelerated moving plate in a rotating system. *J. Magn. Magn. Mater.* **422**, 112–123 (2017). <https://doi.org/10.1016/j.jmmm.2016.08.081>
24. Mohamad, A.Q., Khan, I., Jiann, L.Y., Shafie, S., Isa, Z.M., Ismail, Z.: Heat transfer on rotating second grade fluid through an accelerated plate. *Malays. J. Fundam. Appl. Sci.* **13**(3), 218–222 (2017). <https://doi.org/10.11113/mjfas.v13n3.645>
25. Mohamad, A.Q., et al.: Exact solutions on mixed convection flow of accelerated non-coaxial rotation of MHD viscous fluid with porosity effect. *Defect Diffus. Forum* **399**, 26–37 (2020). <https://doi.org/10.4028/www.scientific.net/DDF.399.26>
26. Krishna, M.W., Ahamad, N.A., Chamkha, A.J.: Hall and ion slip effects on unsteady MHD free convective rotating flow through a saturated porous medium over an exponential accelerated plate. *Alex. Eng. J.* **59**, 565–577 (2020). <https://doi.org/10.1016/j.aej.2020.01.043>
27. Narahari, M., Debnath, L.: Unsteady magnetohydrodynamic free convection flow past an accelerated vertical plate with constant heat flux and heat generation or absorption. *ZAMM J. Appl. Math. Mech.* **93**(1), 38–49 (2013). <https://doi.org/10.1002/zamm.201200008>
28. Hussanan, A., et al.: Unsteady MHD flow of some nanofluids past an accelerated vertical plate embedded in a porous medium. *Jurnal Teknologi* **78**, 121–126 (2016). <https://doi.org/10.11113/jt.v78.4900>
29. Tiwari, R.K., Das, M.K.: Heat transfer augmentation in a two-sided lid-driven differentially heated square cavity utilizing nanofluids. *Int. J. Heat Mass Transf.* **50**, 2002–2018 (2007). <https://doi.org/10.1016/j.ijheatmasstransfer.2006.09.034>
30. Xue, Q.Z.: Model for thermal conductivity of carbon nanotube-based composites. *Phys. B* **368**, 302–307 (2005). <https://doi.org/10.1016/j.physb.2005.07.024>
31. Villinger, H.: Solving cylindrical geothermal problems using the Gaver-Stehfest inverse Laplace transform. *Geophysics* **50**, 1581–1587 (1985). <https://doi.org/10.1190/1.1441848>
32. Stehfest, H.: Algorithm 368: numerical inversion of laplace transforms [D5]. *Commun. ACM* **13**, 47–49 (1970). <https://doi.org/10.1145/361953.361969>

**Open Access** This chapter is licensed under the terms of the Creative Commons Attribution-NonCommercial 4.0 International License (<http://creativecommons.org/licenses/by-nc/4.0/>), which permits any noncommercial use, sharing, adaptation, distribution and reproduction in any medium or format, as long as you give appropriate credit to the original author(s) and the source, provide a link to the Creative Commons license and indicate if changes were made.

The images or other third party material in this chapter are included in the chapter's Creative Commons license, unless indicated otherwise in a credit line to the material. If material is not included in the chapter's Creative Commons license and your intended use is not permitted by statutory regulation or exceeds the permitted use, you will need to obtain permission directly from the copyright holder.

